DOI: 10.1534/genetics.106.069021

The Balance Between the Novel Protein Target of Wingless and the Drosophila Rho-Associated Kinase Pathway Regulates Planar Cell Polarity in the Drosophila Wing

SeYeon Chung,* Sangjoon Kim,*,[1] Jeongsook Yoon,* Paul N. Adler†,[2,3] and Jeongbin Yim*,[3]

**School of Biological Sciences, Seoul National University, Seoul 151-742, Korea and †Biology Department, University of Virginia, Charlottesville, Virginia 22903*

Manuscript received November 29, 2006
Accepted for publication March 14, 2007

ABSTRACT

Planar cell polarity (PCP) signaling is mediated by the serpentine receptor Frizzled (Fz) and transduced by Dishevelled (Dsh). Wingless (Wg) signaling utilizes Drosophila Frizzled 2 (DFz2) as a receptor and also requires Dsh for transducing signals to regulate cell proliferation and differentiation in many developmental contexts. Distinct pathways are activated downstream of Dsh in Wg- and Fz-signaling pathways. Recently, a number of genes, which have essential roles as downstream components of PCP signaling, have been identified in Drosophila. They include the small GTPase *RhoA/Rho1*, its downstream effector *Drosophila rho-associated kinase* (*Drok*), and a number of genes such as *inturned* (*in*) and *fuzzy* (*fy*), whose biochemical functions are unclear. RhoA and Drok provide a link from Fz/Dsh signaling to the modulation of actin cytoskeleton. Here we report the identification of the novel gene *target of wingless* (*tow*) by enhancer trap screening. *tow* expression is negatively regulated by Wg signaling in wing imaginal discs, and the balance between *tow* and the Drok pathway regulates wing-hair morphogenesis. A loss-of-function mutation in *tow* does not result in a distinct phenotype. Genetic interaction and gain-of-function studies provide evidence that Tow acts downstream of Fz/Dsh and plays a role in restricting the number of hairs that wing cells form.

IN most multicellular organisms, epithelial cells form highly organized tissues with cells polarized along their apical/basal axis. Epithelia are also often polarized within the plane of the tissue, which is called planar cell polarity (PCP) or tissue polarity. In recent years, substantial progress has been made in discerning the mechanisms that lead to PCP in Drosophila in several body regions, especially in the wings and the eyes (reviewed in Shulman *et al.* 1998; Adler 2002). In the Drosophila wing, each cell produces a single distally oriented hair. This arises from the polarized assembly of an actin-containing prehair at the distal vertex of each hexagonal wing cell (Wong and Adler 1993). Mutants in PCP signaling have characteristic defects in both the orientation and number of hairs per wing cell (Gubb and Garcia-Bellido 1982; Wong and Adler 1993). In the eye, polarity is reflected in the mirror image arrangement of ommatidia of opposite chiral forms across the dorsal/ventral boundary, the equator. The photoreceptors within each ommatidium are arranged in an asymmetric trapezoidal shape, with the R7/R8 photoreceptor pointing toward the equator and R3 toward the polar side. Mutations in genes that regulate PCP result in failure of ommatidia to acquire the correct chirality and/or failure to rotate properly (Zheng *et al.* 1995; Tomlinson and Struhl 1999; Weber *et al.* 2000).

Using a number of approaches, investigators have identified genes required for the specification of planar cell polarity in Drosophila. This has led to the identification of the Frizzled pathway as a key for the development of tissue polarity (Gubb and Garcia-Bellido 1982; Vinson and Adler 1987; Wong and Adler 1993; Strutt and Strutt 1999; Adler and Lee 2001). Among the key members of this pathway are *frizzled* (*fz*), which encodes a serpentine receptor (Vinson *et al.* 1989); *dishevelled* (*dsh*), which encodes a cytoplasmic protein (Klingensmith *et al.* 1994; Theisen *et al.* 1994; Krasnow *et al.* 1995); and *starry night/flamingo* (*stan/fmi*), which is a cadherin protein with a seven-pass transmembrane domain (Chae *et al.* 1999; Usui *et al.* 1999).

Dsh and Fz family proteins also participate in the Wingless (Wg)/Wnt signal transduction system that regulate a wide variety of developmental events, including cell proliferation and cell fate specification (reviewed in Logan and Nusse 2004). Recent works also have uncovered some common aspects of the canonical Wg-signaling pathway and PCP signaling: The trimeric G-protein $G\alpha_0$-subunit was reported to be required for direct transduction of Fz signals from the membrane to

[1]*Present address:* Department of Molecular Biology and Genetics, School of Medicine, Johns Hopkins University, Baltimore, MD 21205-2185.

[2]*Corresponding author:* Biology Department, Gilmer Hall 245, University of Virginia, Charlottesville, VA 22903. E-mail: pna@virginia.edu

[3]These authors contributed equally to this work.

downstream components in both pathways (Katanaev *et al.* 2005), and a genetic approach based on *fz* alleles revealed that even though the PCP signaling and the canonical Wg signaling are genetically distinct, *fz* controls these two different signaling activities by a common mechanism (Povelones *et al.* 2005). However, Wg and PCP signaling differ in their requirements for more downstream factors such as *armadillo*/β-*catenin* (*arm*/β-*cat*) (Noordermeer *et al.* 1994) and the transcription factor *pangolin*/*Drosophila T cell Factor* (*pan*/*dTCF*) (Brunner *et al.* 1997; van de Wetering *et al.* 1997) for the former, and small GTPase RhoA/Rho1 (Strutt *et al.* 1997), MAP kinase cascade components (Boutros *et al.* 1998; Paricio *et al.* 1999), and the *inturned*/*fuzzy* (*in*/*fy*) group of genes (Park *et al.* 1996; Collier and Gubb 1997) for the latter. The pathways appear to diverge downstream of Dsh (Axelrod *et al.* 1998; Boutros *et al.* 1998).

The PCP signal from Fz/Dsh directs asymmetric cytoskeletal reorganization and polarized cell morphology in part by activating RhoA/Rho1 (Strutt *et al.* 1997) and its downstream effector, Drosophila Rho-associated kinase, Drok (Winter *et al.* 2001). RhoA acts as a molecular switch that gates signaling to downstream targets, both nuclear and cytoskeletal. In eye development, RhoA signals via Jun N-teminal kinase and Jun to regulate PCP-dependent transcription (Strutt *et al.* 1997; Fanto *et al.* 2000; Weber *et al.* 2000). In the wing, RhoA signals via Drok, which functions by regulating myosin II activity via phosphorylating Spaghetti squash (Sqh), a Drosophila homolog of nonmuscle myosin II regulatory light chain (MRLC) (Karess *et al.* 1991; Winter *et al.* 2001). Mutations in *Drok* result in wing cells forming multiple hairs of normal orientation. In the eye, mutations in *Drok* lead to abnormalities in the rotation of ommatidia (Winter *et al.* 2001).

Here we show that the expression of a newly identified gene, *target of wingless* (*tow*), is negatively regulated by a canonical Wg-signaling pathway and that *tow* interacts with *Drok* in PCP signaling. Loss-of-function mutations in *tow* show neither a PCP phenotype nor *wg*-signaling-related defects, but its overexpression leads to wing cells forming multiple hairs of normal polarity much like loss-of-function mutations in *Drok*. We found that Tow is a nuclear protein in pupal wing cells and that *spaghetti squash* (*sqh*) mRNA was downregulated when Tow was overexpressed. This downregulation is presumably at least part of the reason for the Tow overexpression multiple-hair-cell phenotype.

MATERIALS AND METHODS

Drosophila stocks: Alleles used in this study were UAS-*wg* and UAS-$dTCF^{DN}$ (gifts from R. Nusse); *sev-Gal4 UAS-fz* (a recombinant of *sev*-Gal4 and UAS-*fz*, gift from D. Strutt); UAS-*RhoA*, UAS-Rho^{V14}, UAS-*Drok-CAT*, and UAS-*Drok-CAT-KG*, sqh^{AX3} (gifts from L. Luo); dsh^{1}, α-*tub-Drok*, $Drok^{2}$, $RhoA^{72O}$, zip^{1}, zip^{HX62}, ck^{13}, ck^{07130}, and UAS-RedStinger (Bloomington Stock Center). $stan^{VC31}$, a dominant-negative allele of *stan*, was induced by EMS, and it is a recessive lethal. sha^{VB13} is a temperature-sensitive hypomorphic allele of *shavenoid* (*sha*; also called *kojak*) (He and Adler 2002).

Enhancer trap screening: An enhancer trap screen was performed as described by Kim *et al.* (2006).

X-gal staining of third instar larvae: Imaginal discs were dissected from third instar larvae in phosphate-buffered saline (PBS), fixed in 1% glutaraldehyde in PBS for 20 min at room temperature, and washed twice for 10 min with PBTr (0.5% Triton X-100 in PBS). The disc complexes were immersed in 200 μl of X-gal staining solution (10.0 mm $NaH_2PO_4{\cdot}H_2O$/$Na_2HPO_4{\cdot}2H_2O$ [pH 7.2], 150 mm NaCl, 1.0 mm $MgCl_2$, 3.1 mm $K_4[Fe^{II}(CN)_6]$, 3.1 mm $K_3[Fe^{III}(CN)_6]$, 0.3% Triton X-100) adding 8 μl of 50 mg/ml X-gal to dimethylformamide for several hours at 37°. Disc complexes were washed twice for 10 min each with PBTr and mounted in 70% glycerol. LacZ expression patterns were viewed on Nikon microscopes and photographed with an AxioCam camera. Larvae derived from ~7500 new insertions were stained for lacZ expression, and line 4938 was selected since its expression appeared opposite to that of *wg* in the wing discs.

Plasmid rescue and flanking sequence analysis: A total of 1–5 μg of the *tow*-lacZ genomic DNA was fully digested with *Eco*RI or *Sac*II, and the DNA fragments were self-ligated. After precipitation, the ligated DNAs were transformed into *Escherichia coli* strain XL-1 Blue by electroporation. Of the ligated DNAs, the genomic DNA flanking of the *P*-element insertion was selected by an ampicillin-resistant marker.

The flanking DNA was sequenced using either the IR primer (CGA-CGG-GAC-CAC-CTT-ATG-TTA-TTT-CAT-CAT-G) or the A primer (GAG-TTA-ATT-CAA-ACC-CCA-CGG). The sequence was identified using the BLAST program in the database of genomic clones sequenced by the Berkeley Drosophila Genome Project (http://www.fruitfly.org/).

Clonal analysis: Flip-out clones were generated by the Flp-mediated recombination technique (Golic 1991; Xu and Rubin 1993). Clones were induced at 48–60 hr after egg laying (AEL) by heat shock at 37° for 1 hr, and third instar larvae were dissected and fixed. The genotype of the larvae used to make *wg* flip-out clones was *act>y⁺>Gal4, UAS-CD2/UAS-wg; hs-FLP, MKRS/tow-lacZ*.

Immunohistochemistry: Imaginal discs were dissected from third instar larvae, fixed with fixation buffer (0.1 m PIPES, pH 6.9, 1 mm EDTA, 1.0% Triton X-100, 2 mm $MgSO_4$, 1% formaldehyde), blocked in a solution [50 mm Tris–Cl (pH 6.8), 150 mm NaCl, 0.5% NP-40, 5 mg/ml bovine serum albumin (BSA)] and stained overnight at 4° with appropriate antibodies in a washing/incubation solution (50 mm Tris–HCl, pH 6.8, 150 mm NaCl, 0.5% NP-40, 1 mg/ml BSA). After washing several times, secondary antibodies were applied for 2–4 hr at room temperature or on ice. The cuticles were mounted in antifade mounting solution (BioMeda). The fluorescence images were obtained with a confocal microscope system (Zeiss LSM510).

Primary antibodies used in these experiments were rabbit anti-β-gal (Serotec, 1:2000), mouse anti-Wg (4D4, DSHB, 1:10). Secondary antibodies linked to Cy2 or Cy3 were obtained from Amersham Pharmacia Biotech and used in 1:1000.

RNA *in situ* hybridization: *In situ* hybridization of third instar larvae was done as described before (Tautz and Pfeifle 1989). Digoxigenin-labeled antisense RNA probes were synthesized from full-length cDNA of *tow*.

Generation of *tow* mutants: To obtain a deletion mutant of *tow*, we induced imprecise excision of the *P* element in the *tow*-lacZ line. The flanking sequence is occasionally deleted during *P*-element jumping. The source of the transposase in this dysgenic cross was [Δ2-3]*Ki*, and it mobilized P[lacW]

from the insert site. First, *tow*-lacZ homozygous females were crossed to male [Δ2-3]*Ki*, and the male progeny were crossed to balancer virgins (w; TM3/TM6B). Among the progeny, those whose *P* element had jumped out had white eyes; hence we selected male progeny with white eyes, which do not have the *Ki* phenotype. The selected males were balanced with TM3 or TM6B by crossing individually to TM3/TM6B virgins. Of the ~500 lines, one null mutant, tow^{754}, whose deletion range covers the whole open reading frame (ORF) of the *tow* transcript, was confirmed by genomic PCR.

tow^{fz} inversion mutant was created by hs-FLP-mediated inversion. The P/Piggy Bac insertion alleles tow^{d02991} and fz^{f07870} were kindly provided by the Harvard Exelixis Stock Collection. The relevant transposons contain FRT sequences (Parks *et al.* 2004). A recombinant chromosome carrying both insertions was obtained by meiotic crossing over. Male flies that were w *hs-flp;* tow^{d02991} fz^{f07870}*/TM6* were generated and heat-shocked several times during larval and pupal life. These were crossed to *w;* fz^{R53} females and the progeny were screened for phenotypically *fz* flies. Stocks were established from several such flies and salivary gland squashes were performed to confirm the presence of the predicted inversion. The inversion breaks both the *tow* and the *fz* transcription units. It results in a phenotypically null *fz* allele and a *tow* allele that appears to be a biochemical null.

Generation of transgenic flies: Sequencing confirmed that the fly EST GH12583 that encodes Tow carries an intact *tow* gene. We cloned the full-length EST into the pUAST vector (Brand and Perrimon 1993) to generate flies carrying the UAS-*tow* construct. Various Gal4 drivers were used to analyze the consequences of overexpressing Tow.

arm-tow-GFP is a fusion at the C-terminal end of the full-length Tow open reading frame to the N-terminal end of GFP. It was cloned into the pCaSpeR vector with an *armadillo* (*arm*) promoter, and germline transformation was performed by standard methods (Spradling and Rubin 1982).

Actin staining: Pupal wings were stained with rhodamine-labeled phalloidin, as previously described (Wong and Adler 1993).

Mosaic analysis of $Drok^2$ clones: FLP/FRT-mediated recombination was used to generate clones homozygous for $Drok^2$ in the wing via heat-shock-induced recombination 48–72 hr AEL. Homozygous wing clones in newly eclosed adults were visualized using the MARCM system (Lee and Luo 1999) by the presence of the membrane marker mCD8GFP. The genotype used was *y w* $Drok^2$ FRT^{19A}*/tubP-GAL80, hs-FLP,* FRT^{19A}*; UAS-mCD8GFP/+; tubP-Gal4/+*.

Genetic interaction and sectioning of adult eyes: For genetic interaction studies with *sev-Gal4 UAS-fz* (Strutt *et al.* 1997), flies heterozygous for both *sev-Gal4 UAS-fz* and the *tow* mutation were analyzed. Adult heads were cut and fixed overnight in 4% paraformaldehyde solution at 4°, washed three times for 15 min in 0.1 M phosphate buffer (pH 7.2), and postfixed for 1 hr in 1% OsO_4 until the specimen turn black or dark brown. After washing three times for 10 min in distilled water, the samples were dehydrated with ethanol and propylene oxide. Next, the propylene oxide was exchanged with Spurr and embedded in a mold and polymerized for 24 hr at 65°. The block was sectioned into 200- to 300-nm thick slices with an ultramicrotome through the equatorial region of the eye. The slices were stained with 1% Toluidine Blue O on a hot plate for several minutes, and ommatidia were examined for incorrect rotation and chirality. At least five sections from independent eyes were analyzed for each genotype.

Genetic interaction assays using multiple wing hairs: Wings were mounted in Euparal (Asco Labs) or Gary's Magic Mount and examined under bright-field microscopy. The multiple-wing-hair phenotype in Figure 6 and Table 2 was induced by heat shock at 24 hr after puparium formation (APF) at 37° in animals carrying one copy of *hs-Gal4, UAS-tow* and the mutation or transgene of several components in Drok pathway. The multiple-wing-hair phenotype was quantified in the dorsal surface of an area enclosed by the L3 and L4 vein and the first intervein and the imaginary line starting perpendicularly from the tip of second intervein to the L3. Since overexpression of Tow usually causes the wing blade surface to be uneven and wavy, counting the number of multiple hairs was easier in the central region of the wing than in other regions. The number of multiple hair cells was counted and averaged for at least 10 wings/genotype.

Subcellular localization of Tow: *ap-Gal4/+; UAS-RedStinger/ arm-tow-GFP* pupae were fixed in 4% paraformaldehyde in PBS at 4° overnight. UAS-RedStinger line expresses a variant DsRed (red fluorescent protein) with a nuclear localization signal under the control of UAS. The GFP signals were seen without staining or after anti-GFP staining (1:4,000; Molecular Probes, Eugene, OR). The wings were mounted in Prolong Gold Mounting Media (Molecular Probes) and examined in a ATTO CARV confocal unit attached to a Nikon camera.

Northern hybridization: Heat shock was given to pupae of *hs-Gal4/+; UAS-tow/+* flies (at 24 hr APF) at 37° for 40 min two times with a recovery period of 40 min. Total RNA was isolated with Trizol^R (Gifco). Thirty micrograms of total RNA/sample was separated by formaldehyde gel, blotted onto nitrocellulose membrane (Schleicher & Schuell, Keene, NH), and hybridized with ^{32}P-labeled DNA probe specific for *sqh*. The *sqh* fragment was amplified by RT–PCR from wild-type flies using the *sqh*-specific primers *sqh*-RTP1-5′ (AGT-GCA-GCT-GGT-CGA-AAG-TT) and *sqh*-RTP2-3′ (ATT-CGA-GGT-AGT-CGA-ACA-GA).

Western blotting: *hs-Gal4/+; UAS-tow/+* pupae were heat-shocked as described for the Northern blot analyses. Total protein was isolated and analyzed using standard methods. Thirty micrograms of total protein/sample was separated by 4–20% gradient SDS–PAGE gel, blotted onto PVDF membrane, and incubated with anti-Sqh or anti-phospho-Sqh antibody (Cell Signaling).

RESULTS

Identification of Wg-responsive enhancer trap, 4938, inserted at the *tow* locus: To identify novel molecules involved in wing development, we performed an enhancer trap screen (Kim *et al.* 2006). The P[lacW] transposon (Bier *et al.* 1989) was randomly mobilized, and larvae derived from 7500 *P*-element insertions were stained for β-gal expression. Line 4938 was further analyzed because it drove lacZ expression in the wing pouch but not at the dorsal/ventral (D/V) compartment boundary of the wing disc (Figure 1A) where *wg* is expressed. We show below that this enhancer trap is inserted into the *tow* gene and that its expression is identical to that of *tow*.

The pattern of 4938 enhancer trap (*tow*-lacZ hereafter) expression led us to test whether Wg signaling could regulate its expression. First, we induced Wg-expressing flip-out clones using the FLP–FRT system (Golic 1991; Xu and Rubin 1993) and found that the β-gal expression of *tow*-lacZ was repressed nonautonomously in the vicinity of the clones (Figure 1D). The nonautonomy is expected as Wg is secreted and acts on neighboring cells (Zecca *et al.* 1996; Neumann and Cohen 1997) and

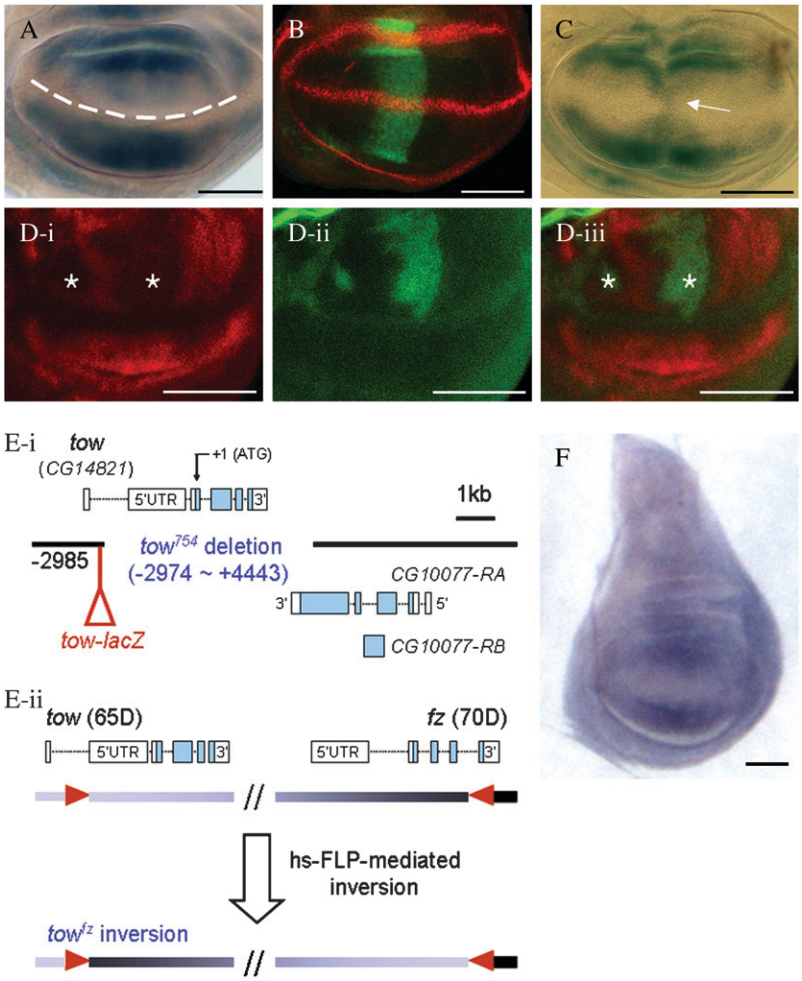

FIGURE 1.—Expression of the *tow* enhancer trap is negatively regulated by Wg signaling in the wing disc. (A) Wild-type *tow*-lacZ expression (X-gal) is found in the whole-wing pouch except the D/V boundary (indicated by white dashed line). (B) Wg expression (red) is not affected by *ptc*-Gal4-driven overexpression of Tow (green). The genotype of the larvae used is *ptc-Gal4/UAS-GFP; UAS-tow/+*. (C) *dpp*-Gal4-driven UAS-$dTCF^{DN}$ derepresses *tow*-lacZ expression at the A/P boundary of the wing (indicated by arrow). The genotype of the larvae is *UAS-*$dTCF^{DN}$*/+; dpp-Gal4/tow-lacZ*. (D) Ectopic expression of Wg (asterisks in D-I and D-iii) represses *tow*-lacZ. (D-i) β-Galactosidase activity of *tow*-lacZ (red). (D-ii) Wg flip-out clones marked by Wg antibody (green). (D-iii) Merged image of i and ii. (E-i) Structure of *tow* gene, enhancer trap *P*-element insertion, and deletion created by imprecise excision. *tow* transcript has a very long 5′-UTR, and 7.4-kb genomic DNA is deleted in the tow^{754} mutant, which removes the whole ORF of the *tow* gene and 160 amino acids of 3′ of the neighboring gene, CG10077. Homozygous tow^{754} mutant flies are normal. (E-ii) tow^{fz} mutant (*tow* and *fz* double mutant) created by hs-FLP-mediated inversion. Homozygous tow^{fz} mutant shows typical *fz* mutant phenotype. *Trans*-heterozygote of tow^{754} and tow^{fz} shows a normal phenotype. (F) *In situ* hybridization to wild-type wing disc using a *tow*-derived RNA probe shows a pattern very similar to that of *tow*-lacZ. (G) Sequence of Tow protein. The residues in red are Gln repeats, and in blue are Pro repeats. Bars in A–D and E, 50 μm.

antibody staining is not sensitive enough to detect levels of ligand known to be biologically active in distant cells (NEUMANN and COHEN 1997; STRIGINI and COHEN 2000). We also utilized the UAS/Gal4 system (BRAND and PERRIMON 1993) to express a dominant-negative form of Drosophila T cell factor (dTCF). The wild-type dTCF protein is a transcription factor activated by Wg signaling, while $dTCF^{DN}$ (VAN DE WETERING *et al.* 1997) inhibits Wg signaling. Expression of $dTCF^{DN}$ in a Decapentaplegic (Dpp) domain [*i.e.*, a stripe that runs perpendicular to the D/V *wg* stripe at the anterior/posterior (A/P) boundary] leads to derepression of β-gal activity of *tow*-lacZ within the Dpp domain (Figure 1C). Thus, Wg signaling negatively regulates the expression of *tow*-lacZ enhancer trap. In other experiments, we found the expression of *wg* was not affected by overexpression or absence of *tow* (Figure 1B). *Drosophila frizzled 2* (*Dfz2*) is a receptor for canonical Wg signaling pathway (BHANOT *et al.* 1996) and is expressed in the wing in a pattern very similar to that of *tow, i.e.*, with the lowest levels found at the D/V boundary (CADIGAN *et al.* 1998). The interaction between Wg and DFz2 plays a crucial role in shaping the Wg morphogen gradient and in determining the response of cells to the Wg signal. We found that the expression of *Dfz2* was also not affected by *tow* (data not shown). Thus, *tow* transcription is a downstream target of Wg signaling.

Sequencing of genomic DNA fragments flanking the insertion showed that the *P* element was inserted into the first intron of a novel gene (CG14821) that we named *target of wingless* (*tow*), which encodes a protein of 347 amino acids. Homologs of *tow* are found in other insects but not in more distantly related organisms. Sequence analysis revealed that there is a highly homologous

gene, *GA13273*, in *Drosophila pseudoobscura* and that it is also very well conserved in other Drosophila species, such as *D. simulans*, *D. yakuba*, *D. erecta*, *D. ananassae*, *D. mojavensis*, and *D. virillis* (their genome sequences are available at http://species.flybase.net/). In addition, the first 60 amino acids in the N terminus show homology to a gene in *Anopheles gambiae*. Tow does not contain informative motifs. However, the sequence is notable for containing eight runs of multiple Gln residues and one Pro-rich region and for being unusually rich in Gln (20.2%) and Pro (10.1%) (Figure 1G).

In situ hybridization to wild-type wing discs using a *tow*-specific probe showed the same expression pattern as 4938 lacZ staining, in that *tow* mRNA was expressed in the wing pouch except at the D/V boundary (Figure 1F).

***tow* null mutant is viable:** To obtain a loss-of-function allele of *tow*, we mobilized the *tow*-lacZ *P* element. We obtained an allele, tow^{754}, which deletes the entire *tow* open reading frame and a part of a neighboring gene, CG10077 (Figure 1E-i). By genomic DNA sequencing, we determined that the 7.4-kb deletion removes the entire *tow* gene except for the first (noncoding) exon and part of the first intron and 160 amino acids of the 3′-end of CG10077-RA, which is the longer of its two transcripts. RT–PCR confirmed that tow^{754} was a null allele as no *tow* mRNA could be detected in tow^{754} homozygous flies (data not shown). Homozygotes of tow^{754} were viable and showed no obvious phenotype. Similar results were obtained with *trans*-heterozygotes of this *tow* mutant and a deficiency for the region.

Since tow^{754} deletes a part of another gene, we made another allele using *hs*-FLP-mediated inversion. We obtained an inversion mutant allele, tow^{fz}, in which a genomic DNA fragment between the first intron of *tow* and the final intron of *fz* was inverted (Figure 1E-ii). Homozygous tow^{fz} flies were also viable and showed a typical *fz* mutant phenotype in the wings and thorax. No *tow* mRNA was detected in homozygous tow^{fz} flies in RT–PCR experiments (data not shown). *Trans*-heterozygotes of tow^{754} and tow^{fz} flies were normal, showing that Tow is nonessential.

Overexpression of Tow causes planar polarity defects manifested by multiple wing hairs: Gain-of-function studies can often give a clue as to the function of a gene and are particularly useful in analyzing functionally redundant genes. We generated transgenic flies, which carried a UAS-*tow* cDNA transgene and crossed them to various Gal4 drivers (Brand and Perrimon 1993). Activation of transcription by Gal4 in *apterous* (*ap*)-expressing cells results in overexpression in thorax and dorsal wing blade. Interestingly, when Tow was overexpressed by the *ap*-Gal4 driver, it caused a disorganization of microchaetae and stunted macrochaetae on the thorax as well as defects in the scutellum (Figure 2B). A disorganized microchaetae phenotype was also seen as a consequence of the misexpression of several planar polarity genes, and gain-of-function screening

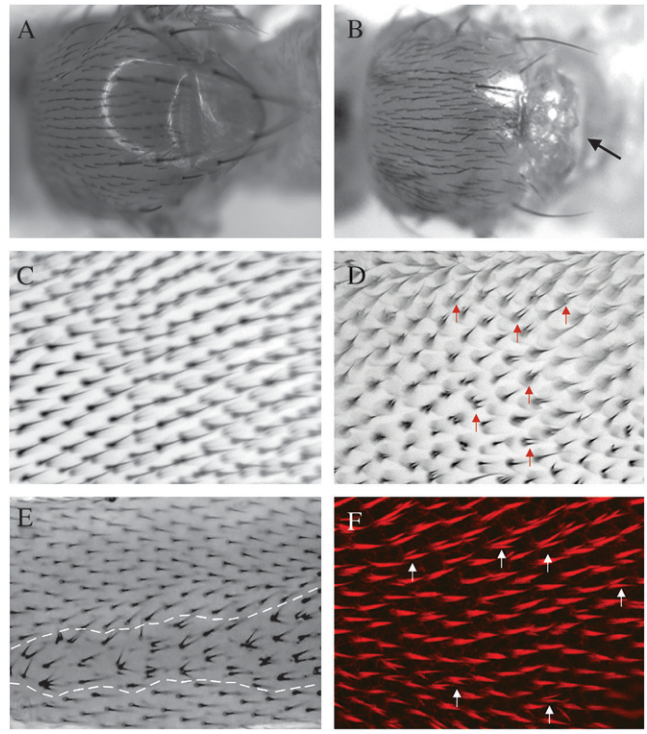

Figure 2.—Overexpression of Tow causes disorganization of microchaetae on the thorax and multiple hairs in the wing. (A and B) Microchaetae phenotype in adult thorax. Anterior is left. (A) Thorax of *ap-Gal4/CyO*. Microchaetae are regularly oriented and point posteriorly. (B) Thorax of *ap-Gal4/+; UAS-tow/+*. Misexpression of Tow results in disorganization of microchaetae and defects in the scutellum (arrow). (C–F) Adult (C–E) and pupal (F) wing phenotypes. In all of the wings, proximal is to the left. (C) Wild-type adult wing. (D) Multiple-hair-cell phenotype of MS1096-Gal4-driven UAS-*tow* adult wing. A few multiple hairs are indicated by red arrows. (E) Multiple hairs on the adult wing in the $Drok^{2}$ mutant clone. The clonal border is marked by a white dashed line. (F) Phalloidin staining of the MS1096-Gal4-driven UAS-*tow* pupal wing reveals multiple F-actin prehairs. White arrows represent several multiple F-actin bundles.

using this bristle defect has been successfully used in finding a novel component of planar polarity (Paricio *et al.* 1999; Feiguin *et al.* 2001). Therefore, this phenotype led us to hypothesize that Tow is also involved in PCP. It is intriguing that a gene whose expression is regulated by Wg signaling could have a function in PCP signaling because the canonical Wg signaling and PCP signaling have been known to diverge into distinct pathways downstream of Dsh (Axelrod *et al.* 1998; Boutros *et al.* 1998).

We overexpressed Tow in the wing using several wing-specific Gal4 drivers, all of which resulted in multiple hair cells (Figure 2D). In wild-type wings, each cell produces a single, distally oriented wing hair, and multiple-hair-cell phenotypes are associated with PCP defects. Most PCP genes, including *fz* and *dsh*, exhibit both stereotypical orientation and multiple-hair-cell defects (Gubb and Garcia-Bellido 1982; Wong and Adler

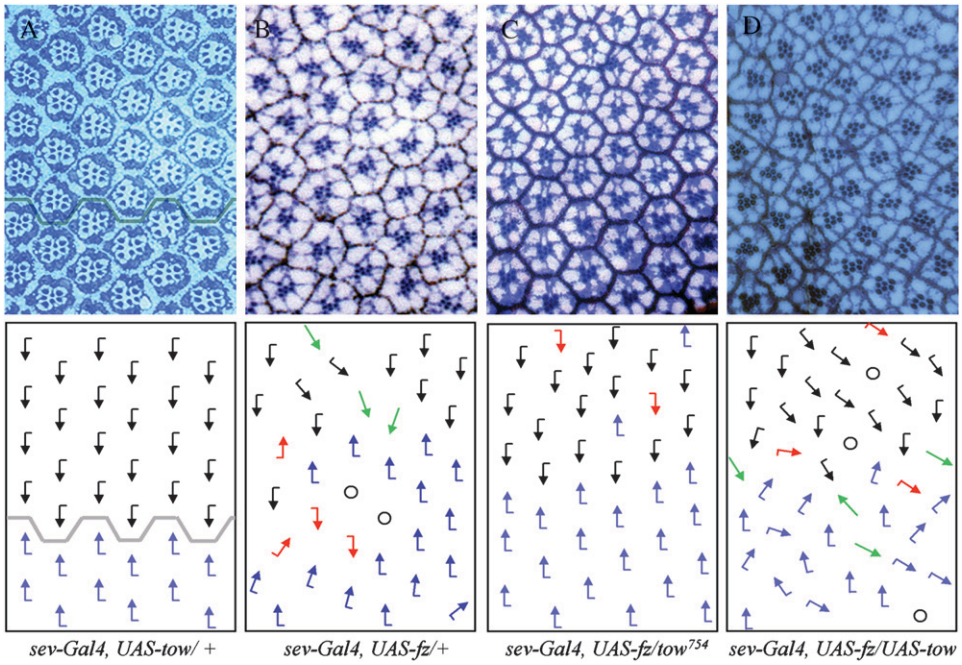

FIGURE 3.—*tow* null mutation dominantly suppresses a polarity-specific Fz gain-of-function phenotype. (A–D) Tangential sections of the equatorial region of adult eyes. Anterior is left, and dorsal is up. Each panel contains eye sections (top) and a schematic of the same area with arrows reflecting ommatidial polarity (bottom). (A) *sev-Gal4/UAS-tow.* It has completely normal eyes. Equator is indicated by gray lines, and it shows ommatidia of normal dorsal and ventral chirality with black and blue arrows, respectively. (B) *sev-Gal4 UAS-fz/+*. Transient *sevenless*-driven overexpression of Fz in the eye results in planar polarity defects. Red arrows represent misrotated ommatidia; green arrows without flags represent symmetrical nonchiral ommatidia. Circles mark unscorable ommatidia, usually due to missing photoreceptors or abnormal morphology. (C) *sev-Gal4 UAS-fz/tow*^{754}. The mutation in *tow* is able to dominantly suppress the gain-of-function *sev-Gal4 UAS-fz* eye phenotype. It is almost completely suppressed. (D) *sev-Gal4 UAS-fz/UAS-tow.* Co-overexpression of Fz and Tow by *sev*-Gal4 results in the enhanced polarity defects. Ommatidia look different in the different genotypes due to fixation or staining variation.

1993), but others such as *Drok* show only the multiple-wing-hair phenotype (WINTER *et al.* 2001; Figure 2E).

To investigate the cellular basis of the Tow overexpression phenotype, we used phalloidin staining to examine the distribution of F-actin during hair morphogenesis. When we used MS1096-Gal4 to drive Tow expression mainly in the dorsal region of the wing (CAPDEVILA and GUERRERO 1994), a majority of wing cells formed more than one F-actin bundle (Figure 2F). Notably, most prehairs maintained a roughly distal orientation. The similarities between the pupal and adult phenotypes indicate that the multiple-hair-cell phenotype of adult Tow-overexpressing wings is likely the result of a failure to restrict F-actin bundle assembly to a single site during prehair formation. Due to the similarity of their multiple-hair-cell phenotypes, we thought it possible that Tow might be involved in the Drok pathway. In addition, MS1096-Gal4-driven Tow overexpression caused extra bristles in the anterior wing margin and in the wing blade near the most distal region, which suggests that ectopic expression of Tow in the wing margin where it is not normally expressed results in formation of extra bristle sense organs in those regions (data not shown).

Tow acts downstream of Frizzled/Dishevelled in planar cell polarity: The proper level of Fz/Dsh signaling is critical for the generation of wild-type PCP, and it has been reported that both overexpression and loss of function of many PCP genes result in polarity defects in the eye (ZHENG *et al.* 1995; STRUTT *et al.* 1997; BOUTROS *et al.* 1998) and the wing (KRASNOW and ADLER 1994; AXELROD *et al.* 1998; GUBB *et al.* 1999; USUI *et al.* 1999; TREE *et al.* 2002). The multiple-hair-cell phenotype of Tow gain of function led us to hypothesize that Tow might also act downstream of Fz/Dsh. To assess the genetic interaction of the Fz pathway and *tow*, we employed two kinds of assays in the eye and in the wing.

In the Drosophila eye, PCP is reflected in the mirror-symmetric arrangement of ommatidial units relative to the dorso-ventral midline, the equator. This pattern is generated posterior to the morphogenetic furrow when ommatidial preclusters rotate 90° toward the equator, adopting opposite chirality, depending on their dorsal or ventral positions (GUBB 1993; Figure 3A). Polarity defects are manifested in the loss of mirror-image symmetry, with the ommatidia misrotating and adopting random chirality or remaining symmetrical (GUBB 1993; THEISEN *et al.* 1994; ZHENG *et al.* 1995; STRUTT *et al.* 1997; BOUTROS *et al.* 1998; WOLFF and RUBIN 1998).

The *sevenless* (*sev*)-driven gain-of-function Fz or Dsh phenotype (*sev-Gal4 UAS-fz* or *sev-Gal4 UAS-dsh*) has previously been used successfully to identify and study new components of the Fz/Dsh planar polarity pathway (STRUTT *et al.* 1997; BOUTROS *et al.* 1998). We employed the same assay to determine if Tow could be a new component of the Fz pathway. *sev*-driven overexpression of Fz in the eye results in planar polarity defects characterized by abnormal ommatidial chirality and misrotation due to overactivation of planar polarity signaling (STRUTT *et al.* 1997; Figure 3B). Null *tow*^{754} flies showed no eye polarity defects and the overexpression of Tow using a *sev* driver also failed to produce an eye phenotype

TABLE 1

Quantification of genetic interactions with the *sev-Gal4 UAS-fz* phenotype

Genotype	Correctly rotated ommatidia (% ± SD)	No. of ommatidia scored
sev-Gal4, UAS-fz/+	44.9 (±9.1)	535
sev-Gal4, UAS-fz/tow^{754}	79.7 (±1.6)	567
sev-Gal4, UAS-fz/tow^{fz}	79.0 (±4.5)	310
sev-Gal4, UAS-fz/fz^{K21}	76.0 (±3.6)	446
arm-fz-GFP/+; sev-Gal4, UAS-fz/+	30.3 (±10.3)	472
arm-fz-GFP/+; sev-Gal4, UAS-fz/fz^{K21}	65.3 (±4.4)	461
arm-fz-GFP/+; sev-Gal4, UAS-fz/tow^{fz}	73.8 (±3.8)	338
arm-fz-GFP/+; tow^{fz}/+	99.7 (±0.6)	320
sev-Gal4, UAS-fz/UAS-tow	26.4 (±6.3)	578

Quantification of genetic interaction of *sev-Gal4 UAS-fz* with *tow*. The quantification of allelic combinations is based on the scoring of five independent eyes per genotype. The percentage figure shown is the average number of correctly oriented ommatidia, with the standard deviation calculated across all eyes of a given genotype scored.

(Figure 3A). However, we found that a null mutation of *tow* acted as a strong dominant suppressor of the gain of function of the *sev-Gal4 UAS-fz* eye phenotype (Figure 3C; Table 1), as is the case for PCP genes such as *RhoA* (Strutt *et al.* 1997).

We confirmed these results using another *tow* allele, *tow^{fz}*. Introduction of a *tow^{fz}* chromosome could also suppress the *sev-Gal4 UAS-fz* eye phenotype (Table 1). Since *tow^{fz}* is a double mutant for *tow* and *fz*, and a *fz* mutant itself can dominantly suppress the *sev*-Gal4-driven Fz overexpression phenotype (Strutt *et al.* 1997; Table 1), we tried to rescue *fz* activity in the *tow^{fz}* mutant by introduction of an *arm-fz-GFP* chromosome (Strutt 2001). The suppression of the *sev-Gal4 UAS-fz* eye phenotype by *tow^{fz}* was still seen when the *arm-fz-GFP* chromosome was present (Table 1). In addition, co-overexpression of Tow and Fz resulted in enhanced polarity defects; notably, the frequency of misrotation of ommatidia was increased (Figure 3D; Table 1). Thus the *sev-Gal4 UAS-fz* phenotype is sensitive to both an increase and a decrease in *tow* dose. These data suggest that Tow could be a downstream target of the Fz pathway or it could function in parallel in eye planar polarity. In addition, two kinds of *tow* alleles showed the same suppression results. Therefore, the deletion of CG10077 in the *tow^{754}* mutant does not seem to affect the genetic interaction with *fz*.

We also examined genetic interactions between *tow* and *dsh*, a downstream effector of Fz. We made use of the *dsh^{1}* allele, which is defective for PCP function without affecting canonical Wg signaling (Axelrod *et al.* 1998; Boutros *et al.* 1998). In a *dsh^{1}* mutant, typical polarity defects such as swirling hair patterns and multiple wing hairs are seen (Wong and Adler 1993; Figure 4A). To

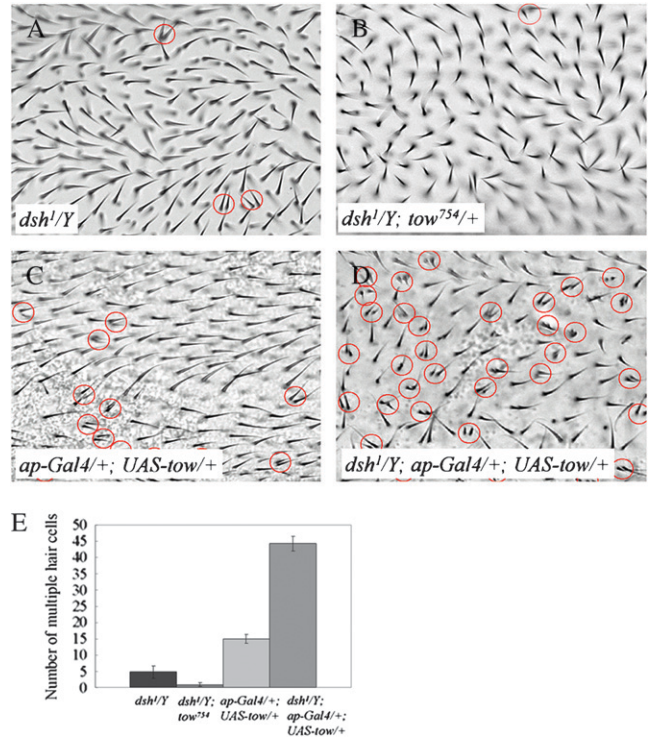

Figure 4.—*tow* mutant suppresses *dsh^{1}* multiple-hair-cell phenotype, and its gain-of-function phenotype is enhanced in a *dsh^{1}* background. (A–D) Representative multiple-hair-cell phenotypes (circled in red) on a dorsal surface of the central region of the adult wing. The genotypes are (A) *dsh^{1}/Y*, (B) *dsh^{1}/Y; tow^{754}/+*, (C) *ap-Gal4/+; UAS-tow/+*, and (D) *dsh^{1}/Y; ap-Gal4/+; UAS-tow/+*. The *dsh^{1}* polarity phenotype looked like it was enhanced because *ap*-driven overexpression of Tow caused the wing blade to be very uneven. (E) The number of multiple hair cells. Error bars represent standard errors. In all of the adult wings, proximal is to the left.

assess the genetic interactions between *dsh* and *tow*, we quantified the multiple-hair-cell phenotype in a defined region, the dorsal surface of the central region of the wing (the region is described in detail in materials and methods).

In *dsh^{1}* hemizygous males, an average of 4.8 cells with multiple hairs were present in this region (Figure 4, A and E). This multiple-hair-cell phenotype was suppressed by the reduction of *tow* dosage, leading to an average of only 0.8 multiple hair cells in the defined region, when one copy of the *tow^{754}* chromosome was introduced (Figure 4, B and E). The polarity of wing hairs in *dsh^{1}* hemizygotes was not affected by *tow* dosage. *ap*-Gal4-driven UAS-*tow* resulted in multiple hairs over the entire dorsal surface of the wing, and in our target region an average of 14.9 cells with multiple hairs were found (Figure 4, C and E). When Tow was overexpressed by *ap*-Gal4 in a *dsh^{1}* hemizygous background, the average number of cells exhibiting multiple hairs was substantially increased to 44.3/wing region (Figure 4, D and E). *ap*-Gal4-driven overexpression of Tow caused the wing blade to be very uneven and wavy, so the polarity

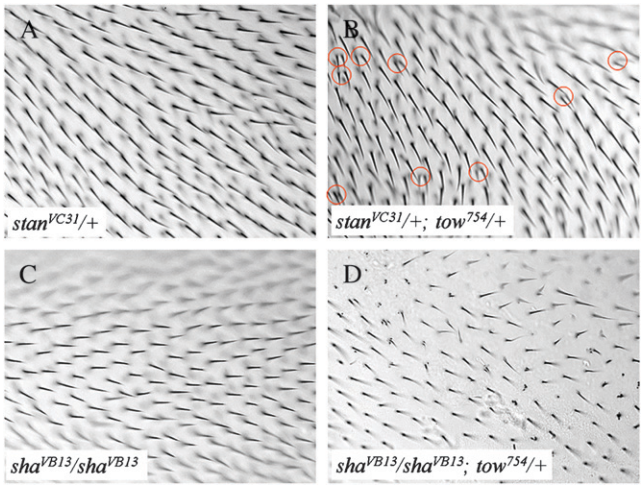

FIGURE 5.—Genetic interaction of *tow* and other PCP components (A–D) Representative wing-hair phenotype of the dorsal compartment of the adult wing. (A) $stan^{VC31}$/+ wing in the anterior region. (B) *Trans*-heterozygotes of tow^{754} and $stan^{VC31}$ showing increased multiple wing hairs. (C) sha^{VB13} homozygous adult wing in the center of the most posterior region. (D) Reduction of *tow* dosage increased number of small hairs and multiple wing hairs in a sha^{VB13} background.

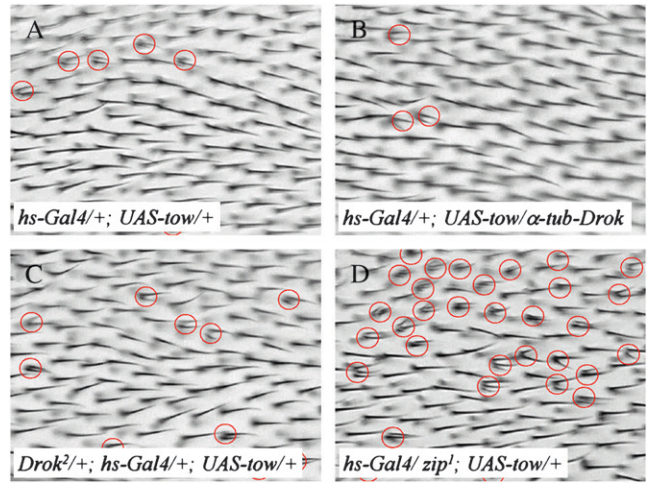

FIGURE 6.—Evidence that Tow genetically interacts with Drok pathway. (A–D) Representative multiple-hair-cellphenotype (circled in red) of various genotypes in a defined region of the adult wing. In A–D, heat shock was given at 37° 24 hr APF. (A) *hs-Gal4/+; UAS-tow/+* wing. (B and C) Overexpression of Drok via a α-*tubP-Drok* transgene results in a reduced number of multiple hairs, and reduction of *Drok* dosage causes an increase in the number of multiple hair cells. (B) *hs-Gal4/+; UAS-tow/*α*-tub-Drok*. (C) $Drok^2$/+; *hs-Gal4/+; UAS-tow/+*. (D) *hs-Gal4/*zip^1*; UAS-tow/+*. *zipper* mutation results in a substantial increase of multiple hairs. In all of the wings, proximal is to the left.

phenotype in dsh^1 looked enhanced. However, when Tow was overexpressed by a weaker driver such as *hs*-Gal4, it was obvious that only the number of multiple wing hairs was increased and no apparent enhancement of polarity phenotype was detected (data not shown). In the control wings of dsh^1*/Y; ap-Gal4/+* or dsh^1*/Y; UAS-tow/+* flies, no remarkable variation of the number of multiple hair cells was observed. We found a similar effect between tow^{fz} and dsh^1 alleles when *fz* activity was rescued by the *arm-fz-GFP* chromosome (data not shown). In a previous study, the overexpression of Drok reduced the average number of multiple hair cells in dsh^1 hemizygotes, and a reduction in *Drok* dose caused an increased number of multiple hair cells, which led to the suggestion that Drok was activated by Fz signaling (Winter *et al.* 2001). We found an opposite dose response between *tow* and dsh^1. Taken together, these experiments suggest that Tow functions downstream of Fz/Dsh perhaps to inhibit Drok activity.

Genetic interaction of *tow* with other PCP genes: To see if *tow* genetically interacts with other known PCP genes, we crossed the tow^{754} null mutant to several PCP mutants and examined the phenotypes of the *trans*-heterozygotes or double homozygotes. The dominant allele of *stan*, $stan^{VC31}$, causes a swirling polarity pattern and a small number of multiple hair cells on the wing. The number of multiple hair cells was increased by a reduction in *tow* dosage (Figure 5, A and B). The introduction of one copy of the tow^{754} null allele also can enhance the phenotype of the *sha* mutant. Mutations in *sha* result in a delay in hair morphogenesis and, in some cells, no hair or only several small hairs form (He and Adler 2002). The morphogenesis of the hair involves temporal control by *sha* and spatial control by the genes of the Fz pathway, and there is a strong genetic interaction between mutations in these genes (Ren *et al.* 2006). *tow* mutation caused an increased number of small hairs and multiple wing hairs in the hypomorphic sha^{VB13} background (Figure 5, C and D). We also looked for interactions with other PCP genes such as *Van Gogh* [*Vang*; also known as *strabismus* (*stbm*)], which encodes a putative membrane protein (Taylor *et al.* 1998; Wolff and Rubin 1998); *fy*, which encodes a novel four-pass transmembrane protein (Collier and Gubb 1997); and *prickle* (*pk*), which encodes a protein with LIM domains (Gubb *et al.* 1999). However, there was no distinct interaction between the *tow* mutant and $Vang^{TBS42}$, a dominant allele of *Vang* (Taylor *et al.* 1998); fy^{JN11}/fy^{JN12}, weak alleles of *fy* (Collier and Gubb 1997); and pk^{D}, a dominant allele of *pk* (Adler *et al.* 2000).

***tow* genetically interacts with the Drok pathway:** Transient overexpression of Tow driven by *hs*-Gal4 with heat shock at 24 hr APF caused the formation of multiple hair cells throughout the wing blade. Once again, the multiple hairs had largely normal polarity. In the flies that carried one copy of both *hs*-Gal4 and UAS-*tow*, an average of 10.9 cells with multiple hairs was found in the defined region (Figure 6A; Table 2). When Drok was simultaneously overexpressed [using a α-*tubP-Drok* transgene (Winter *et al.* 2001)] with Tow, the average number of multiple hair cells was reduced by more than one-half to 4.6/wing region (Figure 6B; Table 2). This suppression was confirmed with co-overexpression of

TABLE 2

Genetic interaction with *tow* gain-of-function phenotype

Genotype	Interaction[a]	Multiple wing hairs/sector		
		Average	Standard error	*N*
hs-Gal4/+; UAS-tow/+	—	10.9	±1.4	10
hs-Gal4/+; UAS-tow/tow^{754}	Suppression	3.2	±1.1	11
hs-Gal4/arm-tow-GFP; UAS-Tow/tow^{754}		5.1	±0.6	20
hs-Gal4/+; UAS-tow/UAS-RhoA	Suppression	2.1	±1.0	10
hs-Gal4/UAS-Drok-CAT; UAS-tow/+	Suppression	5.3	±1.2	11
hs-Gal4/+; UAS-tow/α-tub-Drok	Suppression	4.6	±1.1	11
hs-Gal4/RhoA^{72O}; UAS-tow/+	Enhancement[b]	13.3	±0.9	10
hs-Gal4/UAS-Drok-KG; UAS-tow/+	Enhancement[b]	13.5	±1.3	12
Drok^{2}/+; hs-Gal4/+; UAS-tow/+	Enhancement	24.7	±1.6	14
sqh^{AX3}/+; hs-Gal4/+; UAS-tow/+	Enhancement[b]	13.0	±1.2	12
hs-Gal4/zip^{1}; UAS-tow/+	Enhancement	46.1	±2.8	10
hs-Gal4/zip^{IIX62}; UAS-tow/+	Enhancement	24.4	±1.9	10
hs-Gal4/ck^{13}; UAS-tow/+	Suppression	1.9	±1.1	11
hs-Gal4/ck^{07130}; UAS-tow/+	Suppression	1.5	±0.6	11

Genetic interactions were scored as the effect of the loss of one wild-type copy of the genes or co-overexpression of transgenic constructs tested on the expressivity of the multiple-wing-hair phenotype resulting from heat-shock-induced overexpression of Tow at 24 hr APF.

[a] Statistical significance was determined by Student's *t*-test. Note that, in most cases, the *P*-value is <0.0001, which indicates a highly significant difference.

[b] The *P*-value between two samples is between $0.0001 < P < 0.05$, which represents a likely difference.

the catalytic domain of Drok (*Drok-CAT*) (Winter *et al.* 2001) and Tow by *hs*-Gal4, which resulted in 5.3 multiple hair cells/region (Table 2). Complementary dosage responses were seen with loss-of-function mutations in *Drok*. The presence of a *Drok^{2}* null allele (*Drok^{2}/+*) enhanced the multiple-hair-cell phenotype of *hs-Gal4 UAS-tow* by 2.3-fold to 24.7 multiple hair cells/region (Figure 6C; Table 2). Similarly, when a kinase-dead form of Drok, *Drok-CAT-KG* (Winter *et al.* 2001), which is not a dominant-negative form, was co-overexpressed with Tow, the phenotype was slightly enhanced to 13.5 multiple hair cells/region (Table 2).

Drok is a downstream effector of RhoA/Rho1, which functions as a molecular switch that gates signaling from Fz/Dsh to downstream targets (Strutt *et al.* 1997; Winter *et al.* 2001). The presence of a *RhoA^{72O}* allele (Strutt *et al.* 1997) slightly increased the number of multiple hairs caused by *hs-Gal4 UAS-tow* to 13.3/region (Table 2). On the other hand, co-overexpression of Tow and wild-type RhoA via UAS-*RhoA* (Lee *et al.* 2000) also resulted in a reduced number of multiple hair cells (2.1/wing region, Table 2). A constitutively active form of RhoA, UAS-*Rho^{V14}* (Lee *et al.* 2000), caused lethality when overexpressed by *hs*-Gal4, so we could not examine the effect.

An important substrate of Drok is *sqh*, which encodes the Drosophila homolog of the nonmuscle MRLC. Sqh is phosphorylated by Drok *in vivo* (Karess *et al.* 1991; Jordan and Karess 1997). Reducing the wild-type *sqh* gene dosage from two to one by introducing a single copy of the *sqh^{AX3}* null allele (Jordan and Karess 1997) also slightly enhanced the multiple-wing-hair phenotype caused by Tow overexpression (Table 2).

Zipper (Zip) also functions in hair morphogenesis and interacts with Fz/Dsh (Winter *et al.* 2001). Loss of one copy of the *zip* gene enhanced the *dsh^{1}* and hs-Fz multiple-hair-cell phenotypes, suggesting that myosin II functions positively downstream of Fz/Dsh in hair development. We found that reducing the dose of *zip* substantially enhanced the multiple-hair-cell phenotype caused by overexpression of Tow (Figure 6D, Table 2). This was confirmed for two independent *zip* alleles, *zip^{1}*, a null mutant, and *zip^{IIX62}*, a hypomorph (Table 2).

We also found an interaction with *crinkled* (*ck*), which encodes a myosin VIIA. In the mouse, a mutation in myosin VIIA (*shaker-1* mutant) caused stereocilia disorganization and the formation of multiple stereocilia bundles (Self *et al.* 1998). *ck* was previously found to be involved wing-hair morphogenesis and to interact with Fz/Dsh signaling in Drosophila. Mutations in *ck* cause multiple wing hairs as well as a split-hair phenotype (Gubb *et al.* 1984; Turner and Adler 1998), and a reduction in *ck* gene dose suppressed the *dsh^{1}* multiple-hair phenotype (Winter *et al.* 2001). The genetic interaction of *ck* with components of the Fz/Dsh pathway has opposite effects to that of *zip*, and the seemingly antagonistic relationship between myosin II and myosin VIIA suggested a mechanism in which the balance of the activities or stoichiometry of these two myosins is critical for the common process that they regulate (Winter *et al.* 2001). We also found a complementary genetic interaction of *tow* with these two myosins. Contrary to the enhancement

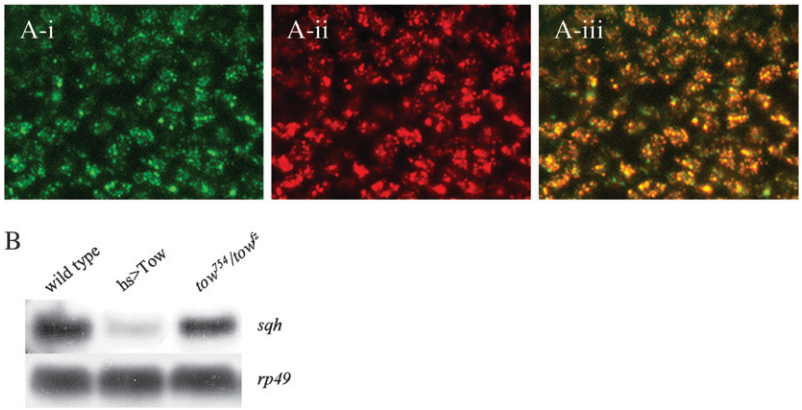

FIGURE 7.—Tow protein is localized in the nucleus, and overexpression of Tow represses *sqh* mRNA. (A) Subcellular localization of Tow in pupal wing cells of *arm-tow*-GFP. (A-i) GFP signal (green) showing subcellular localization of Tow protein. (A-ii) *ap*-Gal4-driven UAS-RedStinger wing, which results in the red fluorescent protein in the nucleus. A-i and A-ii are merged in A-iii. GFP and nuclear signal show the same localization patterns. (B) *hs*-Gal4-driven overexpression of Tow represses the level of *sqh* mRNA.

of the Tow overexpression phenotype by the introduction of the *zip* mutant chromosome, reduction in the *ck* dose suppressed the multiple-wing-hair phenotype due to overexpression of Tow to only one or two multiple hair cells per region (Table 2). This was also confirmed by two independent alleles, ck^{13} and ck^{07130} (Table 2).

Tow is localized in the nucleus in pupal wing cells and overexpression of Tow downregulates the level of *sqh* mRNA: GFP was fused to the C terminus of Tow to generate a tool for studying the subcellular localization of the Tow protein. The *tow*-lacZ signal was uniformly distributed in the pupal wing blade, so we expressed Tow-GFP under the control of the ubiquitous promoter of *arm* (VINCENT *et al.* 1994) and examined *arm*-Tow-GFP distribution in pupal wings at various times between 24 and 36 hr APF. The GFP signal in pupal wings was always found in what we suspected to be nuclei. To confirm this, we colocalized *arm*-Tow-GFP and a nuclear fluorescent protein (using the UAS-RedStinger line, which expresses a variant red fluorescent protein with a nuclear localization signal under the control of UAS). Indeed, the two signals colocalized, consistent with Tow being primarily a nuclear protein in the pupal wing cells (Figure 7A).

Due to the lack of the mutant phenotype for *tow*, we could not test the function of Tow-GFP by simply looking at the rescue of a *tow* mutation. Hence, we expressed Tow-GFP in *hs-Gal4/+; UAS-tow/*tow^{754} flies. The tow^{754} null mutation can suppress the multiple-hair-cell phenotype caused by the *hs*-Gal4-driven overexpression of Tow by about two-thirds (Table 2). Introduction of the *arm-tow-GFP* chromosome slightly but significantly increases the number of multiple hair cells, so we assume that *arm*-Tow-GFP mimics endogenous Tow function. However, we note that we still cannot rule out the possibility that *arm*-Tow-GFP also localized to ectopic sites where Tow is not normally present.

The nuclear localization of Tow-GFP led us to test whether the multiple-wing-hair phenotype caused by Tow overexpression could be due to repression of the mRNA level of one or more components of the Drok pathway. Total RNA was isolated from the *hs-Gal4 UAS-tow* pupae to which heat shock was given 24 hr APF, and Northern hybridization results showed that the mRNA level of *sqh*, a substrate of Drok, was repressed in the Tow-overexpressing flies (Figure 7B). Western blotting experiments confirmed that Sqh protein and phosphorylated Sqh level were also repressed in the Tow-overexpressing flies (data not shown). On the other hand, no difference in mRNA level was detected in homozygous tow^{754} or tow^{fz} mutants (data not shown), or *trans*-heterozygotes of these (Figure 7B), consistent with the normal phenotypes of those flies.

DISCUSSION

A novel gene whose expression is regulated by the canonical Wg-signaling pathway has a function in PCP signaling: *tow* was identified in an enhancer trap screen, and its expression pattern in the wing imaginal disc was the opposite to that of *wg*. The expression of *tow* was negatively regulated by Wg signaling: When Wg was expressed ectopically, *tow* was downregulated nonautonomously, and when Wg signaling was blocked by misexpression of a dominant-negative form of dTCF (VAN DE WETERING *et al.* 1997), the expression of *tow* was derepressed in the Gal4-expressing domain. The expression of *wg* or its receptor *Dfz2* was not affected by *tow*, which suggested that *tow* is a downstream target of Wg signaling. From its expression pattern and the regulation by Wg signaling, we expected that *tow* might function in the Wg-signaling pathway. Our data, however, showed that Tow has little, if any, function in Wg signaling. The only evidence supporting a role for *tow* in Wg signaling was that the overexpression of Tow in the wing resulted in several extra bristles at the anterior wing margin and in the wing blade near the distal margin. The specification of sensory bristle cells is dependent on *wg* activity (PHILLIPS and WHITTLE 1993; COUSO *et al.* 1994). Since the expression of *wg* or *Dfz2* was not affected by the overexpression of Tow, this extra bristle phenotype might be caused by Tow in some way regulating the expression of one or more downstream genes. On

the other hand, surprisingly, we obtained evidence for *tow* acting in Fz-dependent planar cell polarity signaling.

Studies of the canonical Wg-signaling pathway and Fz-dependent polarity pathway have indicated that divergent signaling mechanisms are involved (Axelrod *et al.* 1998; Boutros *et al.* 1998). Although both the Wg- and Fz-signaling pathways require the function of Dsh, they demonstrate differential requirements for more downstream factors. Our study, however, showed that *tow* expression was negatively regulated by Wg signaling in wing discs and that it functioned in the regulation of the actin cytoskeleton and hair morphogenesis during PCP signaling. In both the wing and the eye, the interactions suggested that Tow functioned as a downstream regulator/component of PCP signaling and the Fz/Dsh pathway. The significance of the regulation of *tow* expression by Wg in wing discs for the function of *tow* during hair morphogenesis is unclear as these two events are temporally separated. Further studies will be required to determine this.

Interactions between *tow* and other PCP genes: We tested for genetic interactions between *tow* and other PCP genes and found that the reduction in *tow* dose enhanced the multiple-hair-cell phenotype of a dominant *stan* allele. This interaction is the opposite of what we saw between *tow* and *dsh*. The basis for this difference is unclear but might be due to Tow affecting the expression of different target genes for these two phenotypes. That *tow* mutations could interact with PCP genes by altering gene expression would not be surprising. The PCP system is sensitive to the relative level of components, and interactions were seen previously between PCP genes and mutations in the *grainy head* transcription factor (Lee and Adler 2004). Our experiments provided evidence for *tow* regulating *sgh* expression and this could explain at least part of the interaction with *dsh*.

The *sha* gene encodes a putative actin-binding protein whose expression increases dramatically just prior to hair initiation (Ren *et al.* 2006). Consistent with the expression of *sha* playing a key role in regulating hair initiation, *sha* mutant wing cells either fail to form a hair or have delayed hair formation. Those cells that form delayed hairs produce multiple short ones. Previously, it was found that decreases in PCP gene function enhanced the *sha* mutant phenotype. We found that reduction in *tow* dose also enhanced a *sha* mutant phenotype. This could be due to an indirect effect of *tow* on the PCP pathway and/or to *tow* regulating *sha* expression directly or by an alternative mechanism.

Proper level of Tow is important in regulation of the actin cytoskeleton: Mutations in a number of genes involved in PCP signaling result in multiple-wing-hair phenotypes as well as a swirling pattern of hairs on the Drosophila wing. Drok is thought to act as an effector of small GTPase RhoA and to link Fz/Dsh signaling to the actin cytoskeleton (Winter *et al.* 2001). *Drok* mutations alter only the number of hairs produced and not the hair orientation; thus these two processes likely diverge upstream of Drok.

The gain-of-function phenotype of Tow (distally oriented multiple hairs) suggested that it functioned in the Drok pathway. Genetic interactions revealed that *Drok* and *tow* have an antagonistic relationship. Increasing Drok expression suppresses and decreasing Drok expression enhances the multiple-wing-hair phenotype caused by Tow overexpression. RhoA is upstream of Drok and functions to activate Drok. Thus, it is not surprising that overexpression of RhoA also suppresses the Tow multiple-hair-cell phenotype while mutation of *RhoA* enhances it. The phosphorylation of Sqh/MRLC by Drok leads to Sqh activation and, consistent with this, a reduction in *sqh* dose enhances the Tow multiple-hair-cell phenotype.The two cellular myosin genes *zip* (myosin II) and *ck* (myosin VIIA) also interact with Tow in a manner consistent with the interactions of these genes with *Drok*. These data suggest that the balance between Drok and Tow is important for the regulation of the actin cytoskeleton.

The *arm-tow*-GFP transgene revealed that Tow is localized in the nucleus in pupal wings. From the subcellular localization of Tow, we assumed that it might influence the expression of components involved in the Drok pathway. The overexpression of Tow downregulates *sqh*, a substrate of Drok. This leads to a decrease in the level of Sqh and phosphorylated Sqh protein. This provides a putative mechanism that can explain the multiple-hair-cell phenotype caused by Tow overexpression, which is similar to the *Drok* mutant phenotype. In a *Drok* mutant, the level of phosphorylated Sqh was reduced, indicating that Drok is required for maintaining the proper level of Sqh phosphorylation (Winter *et al.* 2001). Genetic interactions of *tow* with Drok pathway components also fit such a model. The mutation of genes in the Drok pathway enhanced the multiple-hair-cell phenotype caused by Tow overexpression, and the overexpression or the introduction of transgenes of Drok pathway components suppressed the Tow overexpression phenotype. We conclude that the proper level of Tow (and/or the relative level of Tow and Drok) is important in the regulation of the actin cytoskeleton. However, it remains to be resolved whether the downregulation of *sqh* by overexpression of Tow is direct or not. The absence of a *tow* mutant phenotype suggests that there could be other genes whose function in the regulation of *sqh* is redundant with *tow*.

We thank L. Luo, R. Nusse, D. Strutt, the Bloomington Stock Center, and the Harvard Exelixis Stock Collection for providing the fly stocks and the Developmental Studies Hybridoma Bank for the antibody. This research was supported by a grant (M103KV010002 04K2201 00230) from the Brain Research Center of the 21st Century Frontier Research Program funded by the Ministry of Science and Technology, the Republic of Korea, to J.Y. and a grant from the National Institute of General Medical Science (GM-37136) to P.N.A.

LITERATURE CITED

Adler, P. N., 2002 Planar signaling and morphogenesis in Drosophila. Dev. Cell **2:** 525–535.

Adler, P. N., and H. Lee, 2001 Frizzled signaling and cell–cell interactions in planar polarity. Curr. Opin. Cell Biol. **13:** 635–640.

Adler, P. N., J. Taylor and J. Charlton, 2000 The domineering non-aunotomy of *frizzled* and *Van Gogh* clones in the Drosophila wing is a consequence of disruption in local signaling. Mech. Dev. **96:** 197–207.

Axelrod, J. D., J. R. Miller, J. M. Shulman, R. T. Moon and N. Perrimon, 1998 Differential recruitment of Dishevelled provides signaling specificity in the planar cell polarity and Wingless signaling pathways. Genes Dev. **12:** 2610–2622.

Bhanot, P., M. Brink, C. Harryman Samos, J.-C. Hsieh, Y. Wang *et al.*, 1996 A new member of the *frizzled* family from Drosophila functions as a Wingless receptor. Nature **382:** 225–230.

Bier, E., H. Vaessin, S. Shepherd, K. Lee, K. McCall *et al.*, 1989 Searching for pattern and mutation in the Drosophila genome with a P-lacZ vector. Genes Dev. **3:** 1273–1287.

Boutros, M., N. Paricio, D. I. Strutt and M. Mlodzik, 1998 Dishevelled activates JNK and discriminates between JNK pathways in planar polarity and *wingless* signaling. Cell **94:** 109–118.

Brand, A. H., and N. Perrimon, 1993 Targeted gene expression as a means of altering cell fates and generating dominant phenotypes. Development **118:** 401–415.

Brunner, E., O. Peter, L. Schweizer and K. Basler, 1997 *pangolin* encodes a Lef-1 homologue that acts downstream of Armadillo to transduce the Wingless signal in Drosophila. Nature **385:** 829–833.

Cadigan, K. M., M. P. Fish, E. J. Rulifson and R. Nusse, 1998 Wingless repression of *Drosophila frizzled 2* expression shapes the wingless morphogen gradient in the wing. Cell **93:** 767–777.

Capdevila, J., and I. Guerrero, 1994 Targeted expression of the signaling molecule decapentaplegic induces pattern duplications and growth alterations in Drosophila wings. EMBO J. **13:** 4459–4468.

Chae, J., M. Kim, J. H. Goo, S. Collier, D Gubb *et al.*, 1999 The Drosophila tissue polarity gene *starry night* encodes a member of the protocadherin family. Development **126:** 5421–5429.

Collier, S., and D. Gubb, 1997 Drosophila tissue polarity requires the cell-autonomous activity of the *fuzzy* gene, which encodes a novel transmembrane protein. Development **124:** 4029–4037.

Couso, J. P., S. A. Bishop and A. Martinez Arias, 1994 The wingless signaling pathway and the patterning of the wing margin in *Drosophila*. Development **120:** 621–636.

Fanto, M., U. Weber, D. I. Strutt and M. Mlodzik, 2000 Nuclear signaling by Rac and Rho GTPases is required in the establishment of epithelial planar polarity in the Drosophila eye. Curr. Biol. **10:** 979–988.

Feiguin, F., M. Hannus, M. Mlodzik and S. Eaton, 2001 The ankyrin repeat protein Diego mediates Frizzled-dependent planar polarization. Dev. Cell **1:** 93–101.

Golic, K. G., 1991 Site-specific recombination between homologous chromosomes in Drosophila. Science **252:** 958–961.

Gubb, D., 1993 Genes controlling cellular polarity in Drosophila. Dev. Suppl., 269–277.

Gubb, D., and A. Garcia-Bellido, 1982 A genetic analysis of the determination of cuticular polarity during development in *Drosophila melanogaster*. J. Embryol. Exp. Morphol. **68:** 37–57.

Gubb, D., M. Shelton, J. Roote, S. McGill and M. Ashburner, 1984 The genetic analysis of a large transposing element of *Drosophila melanogaster*. The insertion of a *w+ rst+* TE into the *ck* locus. Chromosoma **91:** 54–64.

Gubb, D., C. Green, D. Huen, D. Coulson, G. Johnson *et al.*, 1999 The balance between isoforms of the Prickle LIM domain protein is critical for planar polarity in Drosophila imaginal discs. Genes Dev. **13:** 2315–2327.

He, B., and P. N. Adler, 2002 The genetic control of arista lateral morphogenesis in Drosophila. Dev. Genes Evol. **212:** 218–229.

Jordan, P., and R. Karess, 1997 Myosin light chain-activating phosphorylation sites are required for oogenesis in Drosophila. J. Cell Biol. **139:** 1805–1819.

Karess, R. E., X. J. Chang, K. A. Edwards, S. Kulkarni, I. Aguilera *et al.*, 1991 The regulatory light chain of nonmuscle myosin is encoded by *spaghetti-squash*, a gene required for cytokinesis in Drosophila. Cell **65:** 1177–1189.

Katanaev, V. L., R. Ponzielli, M. Semeriva and A. Tomlinson, 2005 Trimeric G protein-dependent Frizzled signaling in Drosophila. Cell **120:** 111–122.

Kim, S., S. Chung, J. Yoon, K.-W. Choi and J. Yim, 2006 Ectopic expression of Tollo/Toll-8 antagonizes Dpp signaling and induces cell sorting in Drosophila wing. Genesis **44:** 541–549.

Klingensmith, J., R. Nusse and N. Perrimon, 1994 The Drosophila segment polarity gene *dishevelled* encodes a novel protein required for response to the *wingless* signal. Genes Dev. **8:** 118–130.

Krasnow, R. E., and P. N. Adler, 1994 A single Frizzled protein has a dual function in tissue polarity. Development **120:** 1883–1893.

Krasnow, R. E, L. L. Wong and P. N. Adler, 1995 Dishevelled is a component of the *frizzled* signaling pathway in Drosophila. Development **121:** 4095–4102.

Lee, H., and P. N. Adler, 2004 The *grainy head* transcription factor is essential for the function of the *frizzled* pathway in the Drosophila wing. Mech. Dev. **121:** 37–49.

Lee, T., and L. Luo, 1999 Mosaic analysis with a repressible cell marker for studies of gene function in neuronal morphogenesis. Neuron **22:** 451–461.

Lee, T., C. Winter, S. S. Marticke, A. Lee and L. Luo, 2000 Essential roles of Drosophila RhoA in the regulation of neuroblast proliferation and dendritic but not axonal morphogenesis. Neuron **25:** 307–316.

Logan, C. Y., and R. Nusse, 2004 The Wnt signaling pathway in development and disease. Annu. Rev. Cell Dev. Biol. **20:** 781–810.

Neumann, C. J., and S. M. Cohen, 1997 Long-range action of Wingless organizes the dorsal-ventral axis of the Drosophila wing. Development **124:** 871–880.

Noordermeer, J., J. Klingensmith, N. Perrimon and R. Nusse, 1994 *dishevelled* and *armadillo* act in the Wingless signaling pathway in Drosophila. Nature **367:** 80–83.

Paricio, N., F. Feiguin, M. Boutros, S. Eaton and M. Mlodzik, 1999 The Drosophila STE20-like kinase Misshapen is required downstream of the Frizzled receptor in planar polarity signaling. EMBO J. **18:** 4669–4678.

Park, W. J., J. Liu, E. J. Sharp and P. N. Adler, 1996 The Drosophila tissue polarity gene *inturned* acts cell autonomously and encodes a novel protein. Development **122:** 961–969.

Parks, A. L., K. R. Cook, M. Belvin, N. A. Dompe, R. Fawcett, *et al.* 2004 Systematic generation of high-resolution deletion coverage of the Drosophila melanogaster genome. Nat. Genet. **36:** 288–292.

Phillips, R. G., and J. R. S. Whittle, 1993 *wingless* expression mediates determination of peripheral nervous system elements in late stages of *Drosophila* wing disc development. Development **118:** 427–438.

Povelones, M., R. Howes, M. Fish and R. Nusse, 2005 Genetic evidence that Drosophila *frizzled* controls planar cell polarity and armadillo signaling by a common mechanism. Genetics **171:** 1643–1654.

Ren, N., B. He, D. Stone, S. Kirakodu and P. N. Adler, 2006 The shavenoid gene of Drosophila encodes a novel actin cytoskeleton interacting protein that promotes wing hair morphogenesis. Genetics **172:** 1643–1653.

Self, T., M. Mahony, J. Fleming, J. Walsh, S. D. M. Brown *et al.*, 1998 Shaker-1 mutations reveal roles for myosin VIIA in both development and function of cochlear hair cells. Development **125:** 557–566.

Shulman, J. M., N. Perrimon and J. D. Axelrod, 1998 Frizzled signaling and the developmental control of cell polarity. Trends Genet. **14:** 452–458.

Spradling, A., and G. Rubin, 1982 Transposition of cloned P elements into Drosophila germline chromosomes. Science **218:** 341–347.

Strigini, M., and M. Cohen, 2000 Wingless gradient formation in the Drosophila wing. Curr. Biol. **10:** 293–300.

Strutt, D., 2001 Asymmetric localization of Frizzled and the establishment of cell polarity in the *Drosophila* wing. Dev. Cell **7:** 367–375.

Strutt, D. I., U. Weber and M. Mlodzik, 1997 The role of RhoA in tissue polarity and Frizzled signaling. Nature **387:** 292–295.

Strutt, H., and D. Strutt, 1999 Polarity determination in the Drosophila eye. Curr. Opin. Genet. Dev. **9:** 442–446.

Tautz, D., and C. Pfeifle, 1989 A non-radioactive *in situ* hybridization method for the localization of specific RNAs in Drosophila

embryos reveals translational control of the segmentation gene hunchback. Chromosoma **98:** 81–85.

Taylor, J., N. Abramova, J. Charlton and P. N. Adler, 1998 *Van Gogh*: a new Drosophila tissue polarity gene. Genetics **150:** 199–210.

Theisen, H., J. Purcell, M. Bennett, D. Kansagara, A. Syed *et al.*, 1994 *dishevelled* is required during *wingless* signaling to establish both cell polarity and cell identity. Development **120:** 347–360.

Tomlinson, A., and G. Struhl, 1999 Decoding vectorial information from a gradient: sequential roles of the receptors Frizzled and Notch in establishing planar polarity in the Drosophila eye. Development **126:** 5725–5738.

Tree, D., J. M. Shulman, R. Rousset, M. P. Scott, D. Gubb *et al.*, 2002 Prickle mediates feedback amplification to generate asymmetric planar cell polarity signaling. Cell **109:** 371–381.

Turner, C. M., and P. N. Adler, 1998 Distinct roles for the actin and microtubule cytoskeletons in the morphogenesis of epidermal hairs during wing development in Drosophila. Mech. Dev. **70:** 181–192.

Usui, T., Y. Shima, Y. Shimada, S. Hirano, R. W. Burgess *et al.*, 1999 Flamingo, a seven-pass transmembrane cadherin, regulates planar cell polarity under the control of Frizzled. Cell **98:** 585–595.

van de Wetering, M., R. Cavallo, D. Dooijes, M. van Beest, J. van Es *et al.*, 1997 Armadillo coactivates transcription driven by the product of the Drosophila segment polarity gene dTCF. Cell **88:** 789–799.

Vincent, J. P., C. H. Girdham and P. H. O'Farrell, 1994 A cell-autonomous, ubiquitous marker for the analysis of Drosophila genetic mosaics. Dev. Biol. **164:** 328–331.

Vinson, C. R., and P. N. Adler, 1987 Directional non-cell autonomy and the transmission of polarity information by the *frizzled* gene of Drosophila. Nature **329:** 549–551.

Vinson, C. R., S. Conover and P. N. Adler, 1989 A Drosophila tissue polarity locus encodes a protein containing seven potential transmembrane domains. Nature **338:** 263–264.

Weber, U., N. Paricio and M. Mlodzik, 2000 Jun mediates Frizzled-induced R3/R4 cell fate distinction and planar polarity determination in the Drosophila eye. Development **127:** 3619–3629.

Winter, C. G., B. Wang, A. Ballew, A. Royou, R. Karess *et al.*, 2001 Drosophila Rho-associated kinase (Drok) links Frizzled-mediated planar cell polarity signaling to the actin cytoskeleton. Cell **105:** 81–91.

Wolff, T., and G. M. Rubin, 1998 *strabismus*, a novel gene that regulate tissue polarity and cell fate decisions in Drosophila. Development **125:** 1149–1159.

Wong, L. L., and P. N. Adler, 1993 Tissue polarity genes of Drosophila regulates the subcellular location for prehair initiation in pupal wing cells. J. Cell Biol. **123:** 209–221.

Xu, T., and G. M. Rubin, 1993 Analysis of genetic mosaics in developing and adult Drosophila tissues. Development **117:** 1223–1237.

Zecca, M., K. Basler and G. Struhl, 1996 Direct and long-range action of a Wingless morphogen gradient. Cell **87:** 833–844.

Zheng, L., J. Zhang and R. W. Carthew, 1995 *frizzled* regulates mirror-symmetric pattern formation in the Drosophila eye. Development **121:** 3045–3055.

Communicating editor: A. J. Lopez